Microindentation Studies at the Near Surface of Glassy Polymers: Influence of Molecular Weight

F. J. Baltá Calleja,[1] A. Flores,[1] G. H. Michler[2]

[1]*Instituto de Estructura de la Materia, CSIC, Serrano119, 28006 Madrid, Spain*
[2]*Department of Engineering, Institute of Materials Science, Martin-Luther-Universität Halle-Wittenberg, D-06099 Halle/Saale, Germany*

Received 10 November 2003; accepted 17 February 2004
DOI 10.1002/app.20665
Published online in Wiley InterScience (www.interscience.wiley.com).

ABSTRACT: The viscoelastic-plastic properties of various amorphous, glassy polymers [polystyrene (PS), poly(styrene-acrylonitrile) copolymer (SAN), poly(methyl methacrylate) (PMMA), poly(vinyl chloride) (PVC), polycarbonate (PC)] in the micron and submicron range were investigated by means of load-displacement analysis from depth-sensing experiments. Hardness and Young's modulus values decrease rapidly with increasing depth up to a few microns. New data on the glass transition temperature correlation with microhardness are presented. The influence of annealing below the glass transition temperature upon the microhardness for various glassy polymers is pointed out. For PS, the influence of the molecular weight variation and molecular weight distribution on the microhardness is reported. Results are discussed on the basis of an entanglement network model, recently developed to explain the fine structure of crazes in amorphous polymers. © 2004 Wiley Periodicals, Inc. J Appl Polym Sci 93: 1951–1956, 2004

Key words: amorphous polymers; microindentation hardness; glass transition temperature; molecular weight; entanglements

INTRODUCTION

Preceding microhardness studies using the imaging method show that microindentation is a promising technique for the microstructural investigation of semicrystalline polymers and multicomponent systems of known composition.[1–5] Microhardness, H, of semicrystalline and amorphous polymer blends can often be described in terms of an additive system of the independent hardness components.[6,7] In semicrystalline systems, deviations from the additivity law were explained in terms of the change of the nanostructure, level of crystallinity, and nature of the crystal surface of the individual components.[8] Moreover, recent studies in amorphous starblock copolymer/polystyrene blends with lamellar morphology reveal large deviations from the additivity law, showing an additional influence of peculiarities in morphology and micromechanical deformation processes below the indenter tip.[9–11]

Correspondence to: F. J. Baltá Calleja (embalta@iem.cfmac.csic.es).

Contract grant sponsor: Deutscher Akademischer Austauschdienst (DAAD).
Contract grant sponsor: Max–Buchner Forschungsstiftung.
Contract grant sponsor: Dirección General de Investigación; contract grant number: BFM2000-1474.
Contract grant sponsor: Dirección General de Universidades, Ministerio de Educación, Cultura y Deporte.

Microindentation hardness studies on amorphous polymers are not so numerous in contrast to semicrystalline polymers and polymer blends and were mainly carried out by using the imaging technique. These include systems such as poly(naphthalene dicarboxylate) (PEN), polystyrene (PS), poly(methyl methacrylate) (PMMA), and others.[12,13] The application of the depth-sensing method to the study of the surface mechanical properties of glassy polymers was mainly limited to the case of poly(ethylene terephthalate) (PET), PMMA, poly(ether ether ketone) (PEEK), and rubbers.[14–16]

A linear correlation between H, measured at room temperature, and the glass transition temperature for various glassy polymers with dominating single bonds within the main chain was found.[12] A similar linear variation with a different correlating coefficient was recently reported for a series of ethylene–norbornene copolymers.[13] On the other hand, the *in situ* measurement of H as a function of temperature was shown to conveniently detect the glass transition temperature of amorphous polymers.[17]

In a preceding investigation on depth-sensing experiments at the surface of crazed samples of PS, PMMA, poly(styrene-acrylonitrile) copolymer (SAN), and poly(vinyl chloride) (PVC),[15] a remarkable increase of microhardness inside the fibrillated crazes as compared to the bulk microhardness was found. This H increase and the parallel elastic moduli E increase of the fibrils within the crazes (with a ratio $E_{\text{fibril}}/E_{\text{bulk}} \approx 2.6–2.8$)—despite the high microvoid content within the crazes—suggested that the fibrils were highly stressed.

TABLE I
Average Weight and Number Molecular Weight, Polydispersity, Hardness, and Glass Transition Temperature of the Glassy Polymers Investigated

Material	M_w [(g/mol) 10^5]	M_n [(g/mol) 10^5]	M_w/M_n	T_g [°C]	H [MPa]
PS	4.76	1.13	4.2	95[a]	164
SAN 1	2.00	1.00	2.0	104[a]	180
SAN 2	2.49	1.09	2.3	99[a]	178
PMMA 1	1.52	0.92	1.7	116[a]	187
PMMA 2	22.0	10.0	2.5	102[a]	183
PVC 1	1.27	0.55	2.3	66[b]	152
PVC 2	1.81	1.04	1.7	72[b]	146
PC	0.29	0.22	1.3	148[a]	130

[a] From DSC measurements.
[b] From microhardness tests.

Recent studies comparing the crazing behavior of commercial PS and long-chain branched PS at room and elevated temperatures revealed the influence of long-chain branching on the internal structure of the crazes, and thus, on the microhardness.[18,19] The results were interpreted in light of an entanglement network model, reported earlier.[20,21]

The aim of the present article was to complement the previous microindentation investigations on glassy polymers with new examples, concerning the following:

1. The comparison of the micromechanical properties derived from the depth-sensing method in the submicron range with respect to those within the micron range.
2. The correlation between H and the glass transition temperature (T_g).
3. The influence of molecular weight on the microhardness value.

EXPERIMENTAL

Materials

The following commercial samples were investigated: PS and SAN copolymer with 75% styrene and 25% acrylonitrile (BSL AG, Schkopau); PMMA (Röhm GmbH, Darmstadt); PVC (Hüls AG, Marl); and polycarbonate (PC; Bayer AG, Leverkusen). Molecular weight, polydispersity values, and glass transition temperatures are listed in Table I. The T_g values were determined by using both differential scanning calorimetry (DSC) (Perkin Elmer, Norwalk, CT) and microhardness (Shimadzu, Kyoto, Japan) techniques.

In addition, anionically polymerized PS with molecular weights of 10^5, 2.5×10^5, and 4.5×10^5 g/mol, having a polydispersity $M_w/M_n \approx 1.05$ were studied. Finally, the latter sample was mixed with two additional PS materials of lower molecular weights M_w (0.17×10^5 and 0.35×10^5 g/mol) in the amounts of 3, 5, and 10 wt %. It is to be noted that the entanglement molecular weight of PS is of $M_e \approx 0.17 \times 10^5$ g/mol.

Ultramicroindentation hardness

Depth-sensing experiments were carried out in a Shimadzu Ultramicroindentation Tester DUH 202, using a Vickers diamond indenter. The minimum load that can be applied is 0.1 mN with an accuracy of ±1%. The displacement of the indenter is recorded with an accuracy of 10^{-3} μm. On loading, the force is incremented at constant velocity up to P_{max}, held thereafter for a period of time Δt_{hold} of 6 s, and subsequently reduced at the same rate as in the loading cycle. The applied P_{max} varied in the range 0.2–300 mN. With increasing maximum load, the loading rate was also increased between 0.14 and 70.61 mN/s. The penetration depth values of the indenter for the studied polymers varied between ≈ 0.15 and 8 μm. Figure 1 shows a typical loading–hold–unloading curve for the PC sample. The microhardness value H was derived from the penetration depth value at maximum load P_{max} as

$$H = \frac{2P_{max}\sin(\alpha/2)}{d^2} \quad (1)$$

where P_{max} is the force in N; d is the diagonal length of the projected indentation in meters, $d = 7h_{max}$ (see

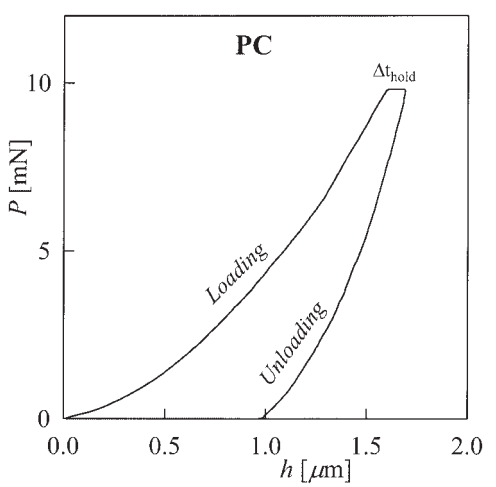

Figure 1 Scheme of a typical load–penetration depth curve for PC. Loading rate: 1.45 mN/s.

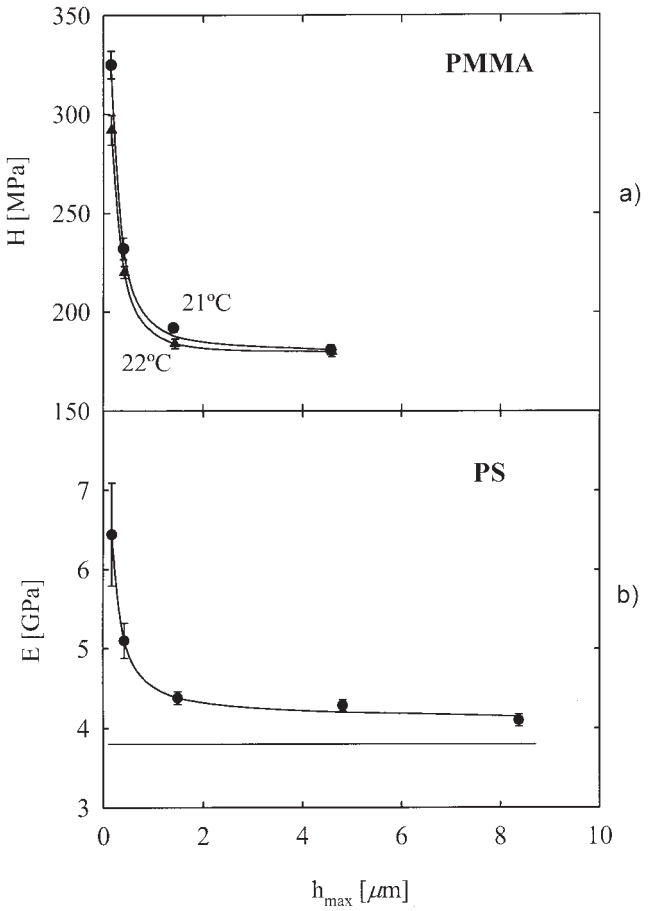

Figure 2 Influence of penetration depth on (a) microhardness for PMMA at 21°C (●) and 22°C (▲), and (b) elastic modulus for PS. The straight line represents the Young's modulus values derived from stress–strain experiments.

Fig. 1); and $\alpha = 136°$ is the included angle between nonadjacent faces of the Vickers pyramid.

Elastic modulus values were derived from the analysis of the unloading curves, following the procedure developed by Doerner and Nix.[22] For further details, see ref. [15].

RESULTS AND DISCUSSION

Dependence of microhardness on penetration depth

In Figure 2 the microhardness data for two test temperatures illustrate the sensitivity of the technique against small shifts of temperature, especially for submicron indentations. All the materials studied (Table I) show the conspicuous dependence of H and E on penetration depth illustrated in Figure 2. Figure 2(a, b) illustrates, as an example, such dependence in the case of PMMA and PS, respectively. It is evident that H (and E) rapidly decreases with increasing penetration depth. For penetration depths larger than 1.5 μm, H (and E) is independent on the penetration depth—we denote this limiting value as H_{bulk}. The continuous straight line in Figure 2(b) represents the Young's modulus derived from stress–strain tests, hence, highlighting the fact that E_{bulk} is reached at penetration depths of a few microns.

TABLE II
Comparison of the Ratio of Microhardness at a Load of 0.2 mN to the Bulk Microhardness for Different Amorphous Polymers

Sample	H (0.2 mN)/H_{bulk}
PS	1.84
SAN 1	1.79
SAN 2	1.73
PMMA 1	1.78
PMMA 2	1.77
PVC 1	1.60
PVC 2	1.57
PC	1.71

The microhardness and elastic modulus increase in the submicron range could be possibly due to the indenter shape effect, in agreement with previous studies in other glassy polymers, carried out by using the same equipment.[14] The ratio of the H value at a load of 0.2 mN (corresponding to a penetration depth of about 0.15 μm), to H_{bulk} is ~ 1.8. The corresponding ratios for the other polymers investigated are listed in Table II. All values of the glassy polymers are in the same range of ~ 1.8; the more ductile samples such as PVC show slightly smaller H (0.2 mN)/H_{bulk} ratios of about 1.6.

Figure 3 also illustrates a similar H decrease with increasing applied load for PS. Here is illustrated as well the H variation when the first 0.5, 1, and 5 μm layers of the top surface, respectively, are removed by

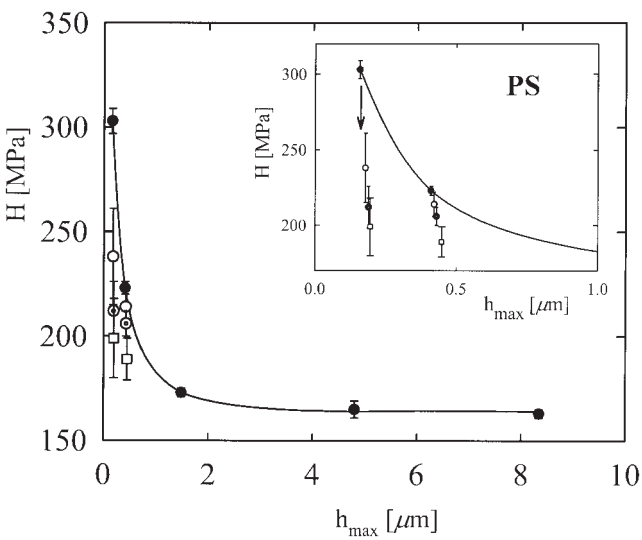

Figure 3 Dependence of microhardness of PS on penetration depth; before (●) and after removal of 0.5 (○), 1 (⊙), and 5 (□) μm thick layers. Inset: enlargement for H-values in the submicron region.

using a Reichert–Jung Microtome MT 6. H was measured again with applied maximum loads of 0.2 and 1 mN. The microhardness of the new microtomed surfaces (after removing the surface layer) shows a dramatic decrease revealing a softening after the surface removal. The smaller values obtained after removing the above-mentioned thin layers could be the result of a rough surface profile due to the cutting process as compared to the smooth original surface.

Correlation of microhardness and glass transition temperature

Similarly to preceding studies in other systems,[17] Figure 4 illustrates the variation of H as a function of temperature for the PS sample. One clearly sees that H decreases with increasing T and the value of T_g can be clearly identified by the sharp bend in the plot. A value of about $T_g \cong 92$°C is derived from this plot, that correlates well with the value calculated from DSC (see Table I). The smaller T_g value from H compared to that from DSC is a result of the fast heating rate used in the DSC determination in contrast to the quasi-static measurement in the case of H.

Figure 5 illustrates the variation of H, measured in the micron range, with T_g for the different polymers studied. A clear rising tendency of H with increasing T_g is observed. This result is in agreement with data reported for a number of polymers and copolymers in the amorphous state, that follow a linear correlation between H and T_g in the form of[12]

$$H = 1.97T_g - 571 \qquad (2)$$

This equation is shown as a dashed straight line in Figure 5. It is to be noted that PC shows a large deviation from eq. (2), as already reported in ref. [12].

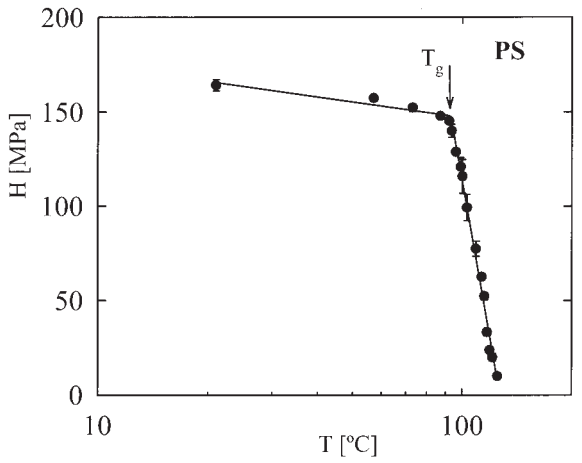

Figure 4 Microhardness as function of temperature for PS. The glass transition value is denoted by an arrow.

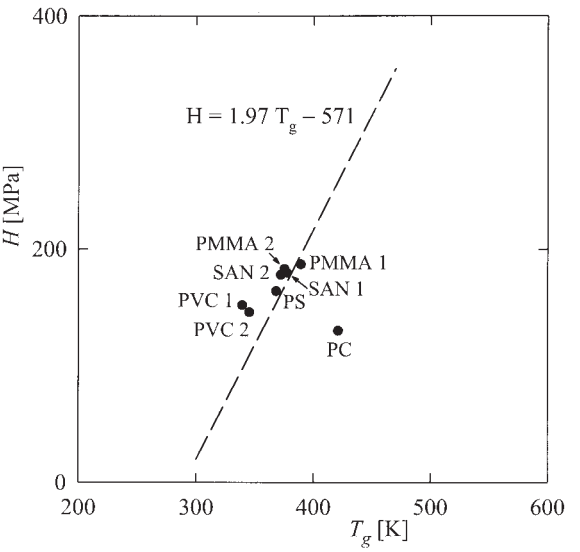

Figure 5 Plot of microhardness versus glass transition temperature for the glassy polymers investigated. The dashed straight line follows eq. 2.

This was associated with the fact that benzene rings dominate the chemical architecture of PC.

Heat treatment of the PC material above T_g, up to 200°C, and subsequent quenching to RT, induces an H decrease of about 15 MPa. On the contrary, annealing of this material at 8–20°C below T_g for 100 h results in an H increase of about 15 MPa. It is noteworthy that much shorter annealing times (5 h) are required for a similar H increase (15 MPa) at 5–15°C below T_g, in the case of SAN. The hardening of glassy polymers is a result of the physical aging of the material and can be correlated with changes in the free volume.[17] The annealing process thus reduces the free volume and enhances H, while quenching induces the reverse process leading to an H decrease.

Influence of molecular weight on microhardness

From Figure 5, one also observes the tendency of H to decrease with increasing molecular weight (see also Table I). This result could be associated with a higher free volume with increasing chain length. To examine the influence of molecular weight on the microhardness, commercial PS was compared with anionically polymerized PS of different M_w. Figure 6 shows the decrease of H with increasing M_w. The commercial PS sample presents a slight deviation from the observed H-tendency, towards smaller H values. It is to be noted that the molecular weight distribution is broader for commercial PS ($M_w = 4.76 \times 10^5$ g/mol, $M_w/M_n = 4.2$) than for the anionic PS samples ($M_w = 10^5$, 2.5×10^5, and 4.5×10^5 g/mol with $M_w/M_n \leq 1.05$). To study the effect of molecular weight distribution on the H values, samples with low $M_w = 0.17$

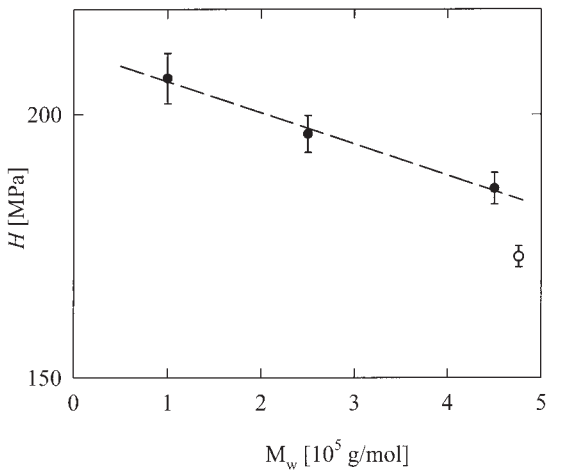

Figure 6 Influence of M_w on the microhardness of PS: anionic polymerized (●) and commercial (○) samples (P_{max} = 10 mN).

$\times 10^5$ g/mol and 0.35×10^5 g/mol were blended, respectively, with anionic high molecular weight PS ($M_w = 4.5 \times 10^5$ g/mol). The influence of the increasing amount of low molecular weight PS from 0 to 10 wt % on H is shown in Figure 7. The H decrease is larger for the 4.5/0.17 blends than for the 4.5/0.35 ones.

Let us discuss the H-molecular weight behavior in light of the entanglement network model that describes the structure of amorphous polymers[20,21] (see Fig. 8). Generally, it is accepted that the macromolecules are entangled above an entanglement molecular weight M_e. However, to develop mechanically strong entanglements (topological, physical connections), a critical molecular weight of $M_c = 2M_e$ has to be surpassed. In the vicinity of M_c, there is a strong increase of mechanical properties (strength, elongation at break, toughness, etc.) with increasing molecular weight. Nonetheless, well above M_c, leveling-off values for the above properties are reached. So far, a correlation between the M_e and T_g and/or microhardness has not been found. There is, however, a correlation between M_e and the internal structure of the microdeformation bands in these glassy polymers and, consequently, in their toughness.[20] The various types of local deformation mechanisms include the formation of crazes with development of fibrils and voids (PS), crazes without fibrils (PMMA), shear bands (PVC), and shear yielding (PC).[20,23] When passing from a morphology of fibrillated crazes to one of homogeneous crazes and to shear bands, ductility and (fracture) toughness increase.

According to the entanglement network model, macromolecules with a characteristic M_e display an entanglement contour length l_e and are characterized by an entanglement distance d_e. Adjacent entanglements are connected to a network with an average mesh size (see Fig. 8). With decreasing M_e, the network mesh becomes smaller and smaller (leading to the transition from fibrillated crazes in PS to homogeneous ones in PMMA and shear yielding in PVC and PC, as mentioned above[20]). Inside the mesh, chain ends, impurities, and low molecular weight molecules are concentrated. As a consequence, the material inside the mesh is mechanically weaker or softer than the entanglement network. This mechanically weak material can be distinguished in deformation tests under the electron microscope as deformed precraze domains in front of the usual, well-developed crazes.[20,24] In our case, in the blends of high M_w anionic PS with low molecular PS (see Fig. 7), the molecular weight of the added PS (M_w = 0.17 and 0.35×10^5 g/mol, respectively) is too low to form strong entanglements. According to our model, this material

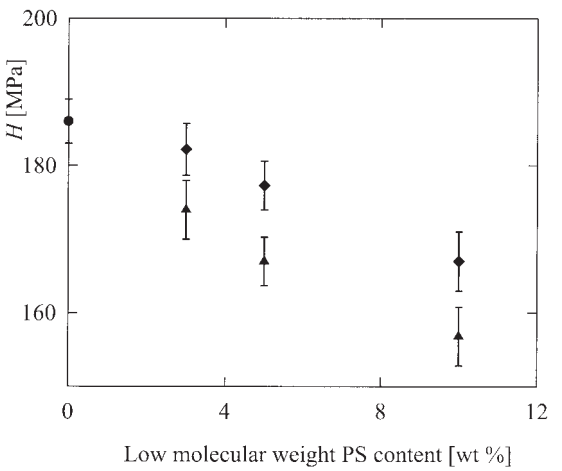

Figure 7 Variation of microhardness of blends of high molecular weight PS ($M_w = 4.5 \times 10^5$ g/mol) (●) with increasing content of two low molecular weight materials (M_w = 0.17 (▲) and 0.35×10^5 g/mol (◆), respectively).

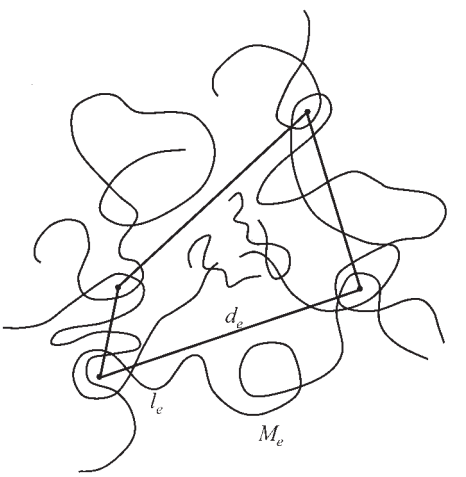

Figure 8 Schematic model of entanglement network in amorphous polymers (ref. 20).

should be located within the meshes of the entanglement network and would contribute to a hardness decrease. The H decrease should be larger with increasing amount of low molecular weight PS (Fig. 7). Moreover, the H decrease is more noticeable for PS macromolecules with $M_w = 0.17 \times 10^5$ g/mol, which are too short to form stable entanglements than the H decrease for PS with $M_w = 0.35 \times 10^5$ g/mol, just above M_c, where macromolecules may form one entanglement per molecule.

By using the above model, a tendency of phase separation between macromolecules of widely different lengths emerges. Such a molecular weight separation or fractionation was discussed for semicrystalline polymers, where macromolecules of different lengths form lamellae of different thicknesses.[25] In blends of PS and PS/PBD block copolymers, larger differences in the molecular weight of the PS segments also give rise to phase separation.[26] According to this concept, segregation (fractionation) of smaller molecules from the larger ones should increase with increasing length of the latter ones (i.e., with increasing width of the molecular weight distribution). As a consequence, larger amounts of separated smaller molecules give rise to segregations of softer molecular aggregates contributing to a decrease of mechanical properties. This would explain the tendency of H to decrease with increasing polydispersity for the studied glassy polymers (see Table I). Moreover, this is also in accordance with the smaller H value of the commercial PS with a broad M_w distribution as compared with the anionic PS with a narrow M_w distribution.

CONCLUSION

1. In the micron range, microhardness and elastic modulus values of the glassy polymers studied, using the depth-sensing method, are shown to remain constant with increasing penetration depth. On the other hand, H and E values in the submicron range ($h < 1.5$ μm) are shown to conspicuously increase with decreasing penetration depth, possibly due to a nonnegligible effect of the indenter tip.

2. The glass transition temperature values derived from microindentation measurements are in good agreement with the T_g values obtained from DSC.

3. The linear correlation between the glass transition temperature and the microhardness was confirmed (except for PC) for the glassy materials investigated (PVC, PS, SAN, and PMMA).

4. Physical aging, induced through annealing, leads to an H increase and occurs at a higher rate in the case of SAN, as compared to PC.

5. The molecular weight increase results in a decrease of microhardness, broader molecular weight distributions leading to lower microhardness values.

6. The entanglement network model, developed to explain precraze structures and internal structure of crazes, can be applied to explain the molecular weight distribution influence upon H. As a consequence, molecular fractionation between macromolecules of very different lengths must be assumed.

We thank M. Ensslen for the careful performance of the microhardness measurements. This project was sponsored by the Deutscher Akademischer Austauschdienst (DAAD) and the Max–Buchner Forschungsstiftung. The authors also acknowledge the Dirección General de Investigación (Grant BFM2000-1474), MCYT, Spain, for the generous support of this investigation. G.H.M. thanks the Dirección General de Universidades, Ministerio de Educación, Cultura y Deporte, Spain, for the award of the Humboldt-Mutis Prize.

References

1. Baltá Calleja, F. J. Trends Polym Sci 1994, 2, 419.
2. Baltá Calleja F. J.; Fakirov, S. Microhardness of Polymers; Cambridge Univ. Press: Cambridge, 2000.
3. Seidler, S.; Koch, T. J Macromol Sci Phys 2002, B41 (4–6), 851.
4. García Gutiérrez, M. C.; Rueda, D. R.; Baltá Calleja, F. J.; Stribeck, N.; Bayer, R. K. Polymer 2003, 44, 451.
5. Awasthi, S. K.; Bajpai, R. Indian J Pure Appl Phys 2001, 39, 795.
6. Berdjane, K.; Berdjane, Z.; Rueda, D. R.; Bénachour, D.; Baltá Calleja, F. J. J Appl Polym Sci 2003, 2046, 89.
7. Baltá Calleja, F. J.; Giri, L.; Ezquerra, T. A.; Fakirov, S.; Roslaniec, Z. J Macromol Sci Phys 1997, B36(5), 655.
8. Cagiao, M. E.; Ania, F.; Baltá Calleja, F. J.; Hirami, M.; Shimomura, T. J Appl Polym Sci 2000, 77, 636.
9. Michler, G. H.; Baltá-Calleja, F. J.; Puente, I.; Cagiao, M. E.; Knoll, K.; Henning, S.; Adhikari R. J Appl Polym Sci 2003, 90, 1670.
10. Baltá Calleja, F. J.; Cagiao, M. E.; Adhikari, R.; Michler, G. H. Polymer, to appear.
11. Adhikari, R.; Michler, G. H.; Cagiao, M. E.; Baltá Calleja, F. J. J Polym Eng, to appear.
12. Fakirov, S.; Baltá Calleja, F. J.; Krumova, M. J Polym Sci, Polym Phys Ed 1999, 37, 1413.
13. Scrivani, T.; Benavente, R.; Pérez, E.; Pereña, J. M. Macromol Chem Phys 2001, 202, 2547.
14. Flores, A.; Baltá Calleja, F. J. Phil Mag 1998, A78(6), 1283.
15. Michler, G. H.; Ensslen, M.; Baltá Calleja, F. J.; Könczöl, L.; Döll, W. Philos Mag 1999, A79, 167.
16. Briscoe, B. J.; Sebastián, K. S.; Sinha, S. K. Philos Mag 1996, A74(5), 1159.
17. Ania, F.; Martínez-Salazar, J.; Baltá Calleja, F. J. J Mater Sci 1989, 24, 2934.
18. García Gutiérrez, M. C.; Michler, G. H.; Henning, S. J Macromol Sci, Phys B 2001, 40, 797.
19. García Gutiérrez, M. C.; Henning, S.; Michler, G. H. J Macromol Sci Phys B 2003, 42, 95.
20. Michler, G. H. Kunststoff-Mikromechanik—Morphologie, Deformations und Bruchmechanismen; Hanser Verlag: München, 1992.
21. Michler, G. H. Plast Kautschuk 1991, 38, 268.
22. Doerner, M. F.; Nix, W. D. J Mater Res 1986, 1, 601.
23. Kausch H. H., Ed.; Crazing of Polymers; Springer-Verlag: Berlin, Heidelberg, 1990; Vol. 2.
24. Michler, G. H. Ultramicroscopy 1984, 15, 81.
25. Michler, G. H.; Brauer, E. Acta Polym 1983, 34, 533.
26. Adhikari, R.; Michler, G. H.; Lebek, W.; Goerlitz, S.; Weidisch, R.; Knoll, K. J Appl Polym Sci 2002, 85, 701.